DPH molecules in βCD and γCD, which is consistent with their inclusion within a CD nanotube, further supported by the difference between the DPH-CD spectra and the spectra of DPH alone in deuterated water (D_2O) and in chloroform ($CDCl_3$), which show different spectral features that are in the range of values for δ of ~6.5 to 7.5 ppm.

Our results suggest that DPH molecules provide a means for the linking of βCD or γCD into rodlike aggregates, or nanotubes, containing about 20 βCDs or 30 γCDs per tube on average. This is shown not only in the formation of the rigid nanotubes and their imaging by STM, but also in the achievement of an isolated, one-dimensional array of conjugated fluorescent molecules that may have the potential to function as a "molecular wire" or a photo switch at a supermolecular level through exciton formation or other processes (*17*).

REFERENCES AND NOTES

1. M. L. Bender and M. Komiyama, *Cyclodextrin Chemistry* (Springer-Verlag, New York, 1978); W. Seanger, *Angew. Chem. Int. Ed. Engl.* **19**, 334 (1980); J. Szejtli, *Cyclodextrins and Their Inclusion Complexes* (Akademiai Kiado, Budapest, 1982); J. Szejtli, *Cyclodextrin Technology* (Kluwer Academic, Dordrecht, 1988); S. Li and W. C. Purdy, *Chem. Rev.* **92**, 1457 (1992).
2. A. Harada, J. Li, M. Kamachi, *Nature* **356**, 325 (1992).
3. G. Wenz and B. Keller, *Angew. Chem. Int. Ed. Engl.* **31**, 197 (1992).
4. A. Harada, J. Li, M. Kamachi, *Nature* **364**, 516 (1993).
5. S. Iijima, *ibid.* **354**, 56 (1991).
6. Aqueous solutions of DPH (15 μM) in CDs (10 mM) were sonicated for 2 hours and then allowed to stand overnight. In the fluorescence measurements, excitation at 325 nm was provided by a He-Cd laser. The emission was selected at 400 to 560 nm with a combination of long-pass and short-pass filters (for the fluorescence lifetime and dynamic anisotropy measurements) and at 420 nm with a monochromator (for the steady-state anisotropy measurements). Scattered light intensity was measured 90° relative to the incident beam at 500 nm for both incident and scattered beams to avoid any absorption by the solutions. The temperature of the samples was kept at 20.0°C. In the STM experiments, two types of instruments (Digital and Burleigh) and tips (Pt-Ir and W) were used to image the nanotube aggregates on highly ordered pyrolytic graphite (HOPG).
7. A. Szabo, *J. Chem. Phys.* **81**, 150 (1984); A. Kawski, *Crit. Rev. Anal. Chem.* **23**, 459 (1993).
8. G. Li and L. B. McGown, *J. Phys. Chem.* **97**, 6745 (1993).
9. J. R. Lakowicz, H. Cherek, B. P. Mailiwal, *Biochemistry* **24**, 376 (1985).
10. P. K. Hansma, V. B. Elings, O. Marti, C. E. Bracker, *Science* **242**, 209 (1988); G. Lee, P. G. Arscott, V. A. Bloomfield, D. F. Evans, *ibid.* **244**, 475 (1989); P. G. Arscott, G. Lee, V. A. Bloomfield, D. F. Evans, *Nature* **339**, 484 (1989).
11. E. D. Cehelnik, R. B. Cundall, J. R. Lockwood, T. F. Palmer, *J. Phys. Chem.* **79**, 1369 (1975).
12. In all three organic solvents, the major peaks in the excitation spectra are red-shifted at the higher DPH concentration (15 μM) relative to the lower concentration (5 μM), and the peak at ~350 nm decreases in intensity. The emission spectra remain similar at the different DPH concentrations.
13. A. Nakajima, *Photochem. Photobiol.* **25**, 593 (1977); R. Weinberger and L. J. Cline Love, *Spectrochim. Acta* **40A**, 49 (1984); G. Li and L. B. McGown, unpublished results.
14. J. B. Birks, *Photophysics of Aromatic Molecules* (Wiley, New York, 1970), chap. 11; M. Orrit and P. Kottis, *Adv. Chem. Phys.* **74**, 1 (1988).
15. We obtained ^1H NMR (500 MHz) spectra with a Varian Unity 500 NMR Spectrometer in the Duke University NMR Spectroscopy Center. It was necessary to saturate the aqueous CD solutions with DPH (<1.0 mM) in order to obtain any signal. The solutions were centrifuged to remove precipitates and allowed to equilibrate overnight. The DPH concentration was too low in the solutions for observation of spectral fine structure. The spectra of the DPH-CD solutions were scanned from 19,000 to 30,000 times. The spectra of saturated DPH in D_2O and 1.0 mM DPH in $CDCl_3$ with no CD were also measured. The solution temperature was maintained at 20.0°C. The HOD water line was nulled by presaturation with a 1-s, low-power pulse from the transmitter to increase the dynamic range.
16. F. A. Bovey, L. Jelinski, P. A. Mirau, *Nuclear Magnetic Resonance Spectroscopy* (Academic Press, New York, ed. 2, 1988); E. Kolehmainen, *J. Colloid Interface Sci.* **127**, 301 (1989).
17. C. A. Mirkin and M. A. Ratner, *Annu. Rev. Phys. Chem.* **43**, 719 (1992).

18. We are grateful to L. A. Coury Jr. for helpful discussion of the STM results, to R. A. MacPhail for valuable comments, and to A. A. Ribeiro for assistance with the NMR experiments and interpretation. This work was supported by the Division of Chemical Sciences, Office of Basic Energy Sciences, Office of Energy Research, U.S. Department of Energy (grant DE-FG0588-ER13931), and by the Environmental Protection Agency (grant R817127-01).

19 November 1993; accepted 9 February 1994

Binding and Suppression of the Myc Transcriptional Activation Domain by p107

Wei Gu, Kishor Bhatia, Ian T. Magrath, Chi V. Dang, Riccardo Dalla-Favera*

An amino-terminal transactivation domain is required for Myc to function as a transcription factor controlling cell proliferation, differentiation, and apoptosis. A complementary DNA expression library was screened with a Myc fusion protein to identify proteins interacting with this domain, and a clone encoding the Rb-related p107 protein was isolated. The p107 protein was shown to associate with Myc in vivo and to suppress the activity of the Myc transactivation domain. However, mutant forms of Myc from Burkitt lymphoma cells, which contain sequence alterations in the transactivation domain, were resistant to p107-mediated suppression. Thus, disruption of a regulatory interaction between Myc and p107 may be important in tumorigenesis.

The *myc* proto-oncogene codes for a ubiquitously expressed nuclear phosphoprotein that functions as a transcriptional regulator controlling cell proliferation, differentiation, and apoptosis (*1*). Structural alterations of the *myc* locus, caused by chromosomal translocation, amplification, retroviral insertion, or retroviral transduction, are consistently associated with tumorigenesis in different species (*1*).

The expression of *myc* is tightly controlled at multiple levels, including transcription initiation and elongation and mRNA stability (*1*). Less is known about the mechanisms regulating Myc protein function. In vivo, Myc is found mainly in heterodimeric complexes with the related protein Max, and this interaction is mediated by helix-loop-helix (HLH) and leucine zipper (LZ) domains present at the COOH-terminus of both proteins (*2*). The Myc-Max complexes stimulate transcription (*3*) and cell proliferation (*4*), whereas Max-Max homodimers or heterodimers formed

W. Gu and R. Dalla-Favera, Division of Oncology, Department of Pathology, and Department of Genetics and Development, College of Physicians and Surgeons, Columbia University, New York, NY 10032, USA.
K. Bhatia and I. T. Magrath, Pediatric Oncology Branch, National Cancer Institute, Bethesda, MD 20892, USA.
C. V. Dang, Departments of Medicine and Cell Biology and Anatomy, and The Johns Hopkins Oncology Center, Johns Hopkins School of Medicine, Baltimore, MD 21205, USA.
*To whom correspondence should be addressed.

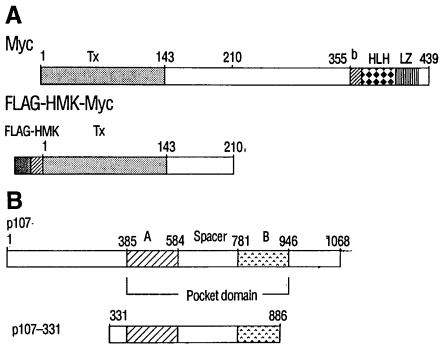

Fig. 1. Identification of proteins associated with the NH_2-terminal domain of Myc. (**A**) Schematic of normal Myc and the fusion protein (FLAG-HMK-Myc) used for screening the cDNA expression library. Tx, transcriptional activation domain. (**B**) Schematic of full-length p107 and of the protein (p107–331) predicted from the sequence of the positive cDNA clone. This clone codes for most of the pocket domain.

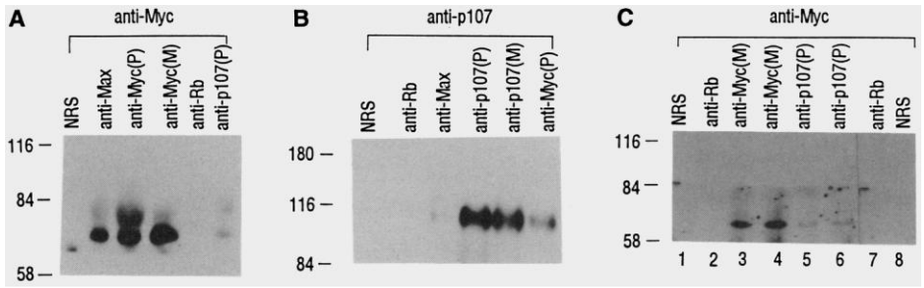

Fig. 2. Association between Myc and p107 in vivo. (**A**) Immunoprecipitates obtained with antibodies to p107 contain Myc. Immunoblot analysis of immunoprecipitates from CB33-SVMyc cells obtained with normal rabbit serum (NRS), a polyclonal antibody to Max (anti-Max), a polyclonal antibody to Myc [anti-Myc(P)], a monoclonal antibody to Myc [anti-Myc(M)], an antibody to Rb (anti-Rb), or a polyclonal antibody to p107 [anti-p107(P)]. (**B**) Immunoprecipitates obtained with antibodies to Myc contain p107. Immunoblot analysis of immunoprecipitates from CB33-SVMyc cells obtained with NRS, anti-Rb, anti-Max, anti-p107(P), monoclonal antibody to p107 [anti-p107(M)] or anti-Myc(P). The immunoblot was developed with anti-p107(P). (**C**) Myc-p107 interaction in cell lines containing physiologic levels of Myc. Immunoblot analysis, done as in (A), of immunoprecipitates from the Bjab (lanes 1, 2, 3, 5) and EW-36 (4, 6, 7, 8) cell lines. Molecular sizes are indicated in kilodaltons.

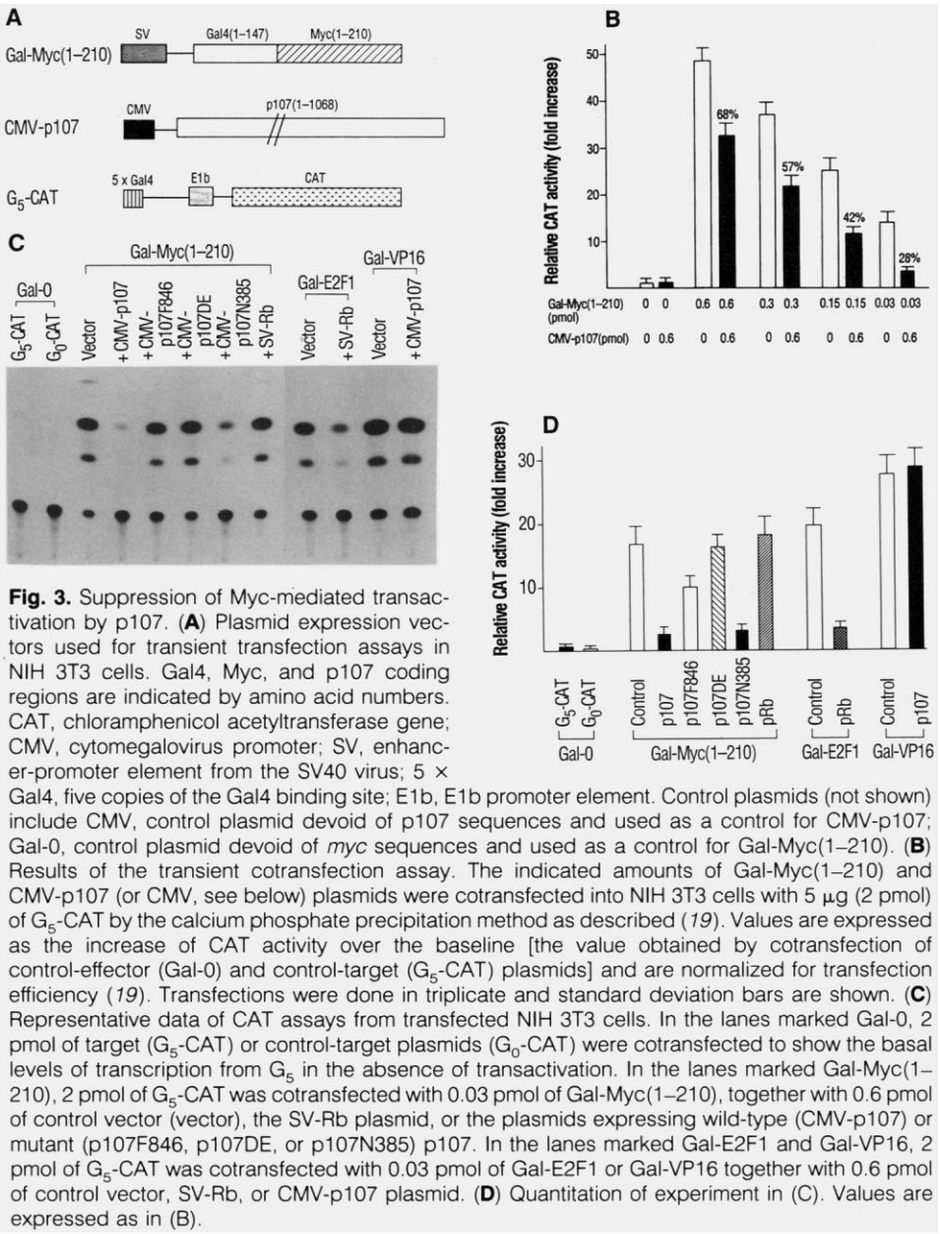

Fig. 3. Suppression of Myc-mediated transactivation by p107. (**A**) Plasmid expression vectors used for transient transfection assays in NIH 3T3 cells. Gal4, Myc, and p107 coding regions are indicated by amino acid numbers. CAT, chloramphenicol acetyltransferase gene; CMV, cytomegalovirus promoter; SV, enhancer-promoter element from the SV40 virus; 5 × Gal4, five copies of the Gal4 binding site; E1b, E1b promoter element. Control plasmids (not shown) include CMV, control plasmid devoid of p107 sequences and used as a control for CMV-p107; Gal-0, control plasmid devoid of *myc* sequences and used as a control for Gal-Myc(1–210). (**B**) Results of the transient cotransfection assay. The indicated amounts of Gal-Myc(1–210) and CMV-p107 (or CMV, see below) plasmids were cotransfected into NIH 3T3 cells with 5 μg (2 pmol) of G_5-CAT by the calcium phosphate precipitation method as described (*19*). Values are expressed as the increase of CAT activity over the baseline [the value obtained by cotransfection of control-effector (Gal-0) and control-target (G_5-CAT) plasmids] and are normalized for transfection efficiency (*19*). Transfections were done in triplicate and standard deviation bars are shown. (**C**) Representative data of CAT assays from transfected NIH 3T3 cells. In the lanes marked Gal-0, 2 pmol of target (G_5-CAT) or control-target plasmids (G_0-CAT) were cotransfected to show the basal levels of transcription from G_5 in the absence of transactivation. In the lanes marked Gal-Myc(1–210), 2 pmol of G_5-CAT was cotransfected with 0.03 pmol of Gal-Myc(1–210), together with 0.6 pmol of control vector (vector), the SV-Rb plasmid, or the plasmids expressing wild-type (CMV-p107) or mutant (p107F846, p107DE, or p107N385) p107. In the lanes marked Gal-E2F1 and Gal-VP16, 2 pmol of G_5-CAT was cotransfected with 0.03 pmol of Gal-E2F1 or Gal-VP16 together with 0.6 pmol of control vector, SV-Rb, or CMV-p107 plasmid. (**D**) Quantitation of experiment in (C). Values are expressed as in (B).

by Max and Mad, another HLH-LZ protein, act as transcriptional repressors (*3–5*). The activity of Myc-Max complexes requires a transcriptional activation domain present at the NH_2-terminus of Myc, but absent from Max (*2–4, 6*). In other transcription factors, the activity of the transcriptional activation domains appears to be regulated by specific protein-protein interactions (*7*). However, no such interaction has been identified for Myc, because an association between Myc and the retinoblastoma (Rb) tumor suppressor protein identified in vitro has not been confirmed in vivo (*8*). The importance of the Myc transactivation domain is supported by the observation that the corresponding sequences are frequently mutated in *myc* oncogenes activated by chromosomal translocations in Burkitt lymphoma and mouse plasmacytoma (*9*).

To identify proteins associated with the Myc NH_2-terminal domain, we screened a λ-gt11 complementary DNA (cDNA) expression library from a B cell lymphoma cell line (Daudi) with a ^{32}P-labeled Myc fusion protein consisting of the NH_2-terminal 210 amino acids of Myc linked to a heart muscle kinase (HMK) domain (for labeling) and a FLAG domain (epitope for immune purification) (Fig. 1A) (*10*). Five distinct signals were identified after primary screening of 3 × 10^6 phage plaques. After plaque purification, one positive clone displayed a strong interaction with the probe containing the NH_2-terminal Myc sequence, but not with a probe containing the COOH-terminal half of Myc. Further analysis of this cDNA insert revealed that it was identical in sequence to a portion of the gene coding for p107, a growth suppressor protein related to Rb (*11*). Like Rb, p107 associates with viral transforming proteins, including adenovirus E1A and SV40 large T antigen (*11*). In particular, the cDNA sequence corresponded to almost the entire "pocket" domain of p107 (Fig. 1B), a region essential for viral protein binding as well as for cell cycle regulation and growth suppression (*12*). Thus, the NH_2-terminal half of Myc associates with the pocket domain of p107 in vitro.

To determine whether p107 and Myc associate in vivo, we performed immunoprecipitation experiments. Extracts from CB33-SV-Myc2.3 cells, an Epstein-Barr virus (EBV)–transformed lymphoblastoid cell line, engineered to express high levels of Myc from a transfected gene (*4, 13*), were first immunoprecipitated at low stringency with an antibody to p107 (anti-p107) and then immunoblotted with an antiserum to Myc (anti-Myc) (*14*). Immunoprecipitates obtained with antibodies to Myc or to Max (anti-Max) were used as positive controls for the procedure and for the detection of

Myc-Max complexes, respectively. We also analyzed immunoprecipitates obtained with an antiserum to Rb (anti-Rb) so that we could compare the binding of Myc to the related p107 and Rb proteins in vivo. The two normal (67- and 65-kD) Myc proteins were detectable in immunoprecipitates obtained with antibodies to p107, Myc, and Max, but not in those obtained with control antiserum (Fig. 2A). Notably, Myc was not detectable in immunoprecipitates generated by anti-Rb, although expression of Rb in these cells was confirmed by immunoprecipitation analysis (*15*).

To corroborate these findings, we did the reciprocal experiment: We searched for p107 in immunoprecipitates generated by anti-Myc. We detected p107 in immunoprecipitates obtained with anti-Myc and anti-p107 (positive control), but not in those obtained with an anti-Rb or with control serum (Fig. 2B). Notably, p107 was also detectable in immunoprecipitates obtained with the anti-Max. As no direct interaction has been detected between p107 and Max in vitro (*16*), this result suggests that p107 can bind Myc when Myc is complexed with Max. Analogous results were obtained with immunoprecipitates from two cell lines (Bjab and EW-36) (*17*) not transfected with Myc expression plasmids (Fig. 2C), indicating that the Myc-p107 interaction can occur under physiological conditions. The detection of p107 in immunoprecipitates generated by anti-Max—together with the fact that in vivo most Myc molecules are complexed with Max (*2*, *5*)—suggests that at least some p107 is bound, via Myc, to Myc-Max complexes.

To determine the functional consequences of p107 binding, we studied whether p107 affected the transactivation activity of Myc. We cotransfected a p107 expression plasmid with a plasmid carrying NH_2-terminal Myc sequences fused to the yeast Gal4 DNA binding sequences into NIH 3T3 cells and assayed transcription from a reporter gene linked to Gal4 binding sites (Fig. 3A) (*18*, *19*). Cotransfection of the p107 plasmid suppressed the activity of the Myc transactivation domain (Fig. 3B). The suppression was dose-dependent; substantial suppression (68% residual transactivation activity) was already detectable at equimolar input of the p107 and Myc plasmids, and strong suppression (15 to 28% in different experiments) was seen at a 20:1 ratio of the plasmids (Fig. 3). The p107 pocket domain was both necessary and sufficient for suppression, as mutants (*12*) carrying point mutations (p107F846) or deletions of the entire domain (p107DE) were impaired in their suppressive activity, whereas a deletion mutant (p107N385) retaining only the pocket domain was active. We also found that Rb was completely inactive in suppressing Myc transactivation although, as expected (*7*), it could suppress the E2F transactivation domain. Finally, p107 suppressed Myc but not the viral VP16 transactivation domain (Fig. 3, C and D) (*15*). Analysis of Myc deletion mutants (*18*, *20*) in the same transactivation assay indicated that the minimal Myc domain previously identified (*18*) as sufficient for transactivation (amino acids 41 to 103) also mediates suppression by p107 (*21*). Indirectly, this result also suggests that p107 binds to this same domain. Thus, these results indicate that Myc suppression by p107 is specific and requires the same functional domain (pocket) of p107 that mediates its growth suppressive effects.

Multiple point mutations in the sequences coding for the Myc transactivation domain are common in *myc* oncogenes activated by chromosomal translocations in human lymphomas and mouse plasmacytomas (*9*). These mutations appear to cluster within the minimal domain necessary for transactivation and suppression by p107 (*9*). We tested whether mutant Myc proteins derived from three Burkitt lymphoma (BL) cell lines (P3HR1, ST486, and CA46; Fig. 4A) (*22*) displayed abnormal behavior in p107 binding or suppression. The Myc-p107 complex was detectable in these three BL lines by the immunoprecipitation assay (*16*). Because only the mutant Myc protein is expressed in these cell lines (*23*), this result indicates that the mutations do not eliminate Myc-p107 binding, although variations in the affinity of binding of the two proteins could be missed by the nonquantitative two-step assay. In contrast, marked differences were observed between wild-type Myc and the BL-derived mutant Myc proteins in the transactivation assay (Fig. 4, A and B). Although all three mutants displayed transactivation activity comparable with that of wild-type Myc, they were substantially less responsive to p107-induced suppression. Comparative analysis of titration curves generated by varying the ratio of p107 to Myc expression plasmids confirmed that the mutants were virtually unresponsive to p107-induced suppression (Fig. 4C).

The mechanism by which p107 suppresses the Myc transactivation activity remains to be elucidated. It is possible that p107 prevents Myc or the Myc-Max complex from binding DNA. Alternatively, p107 may switch Myc from a positive to a negative regulator, analogous to the action of Rb on E2F (*24*). Finally, because the Myc transactivation domain interacts with components of the basal transcrip-

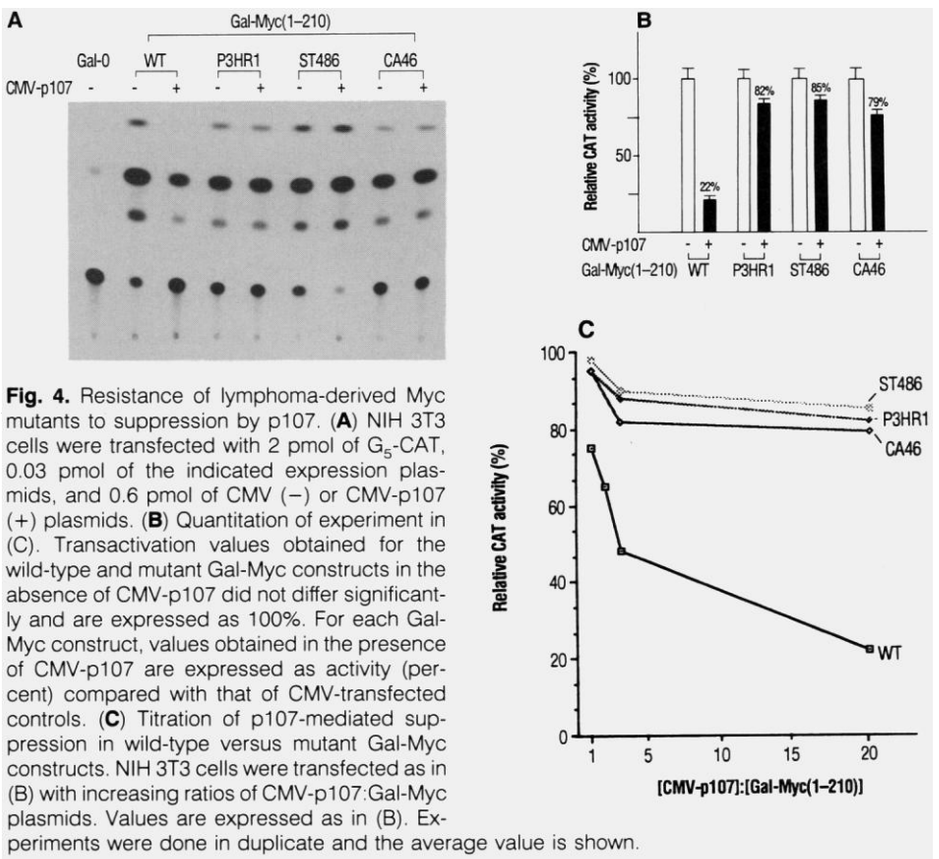

Fig. 4. Resistance of lymphoma-derived Myc mutants to suppression by p107. (**A**) NIH 3T3 cells were transfected with 2 pmol of G_5-CAT, 0.03 pmol of the indicated expression plasmids, and 0.6 pmol of CMV (−) or CMV-p107 (+) plasmids. (**B**) Quantitation of experiment in (C). Transactivation values obtained for the wild-type and mutant Gal-Myc constructs in the absence of CMV-p107 did not differ significantly and are expressed as 100%. For each Gal-Myc construct, values obtained in the presence of CMV-p107 are expressed as activity (percent) compared with that of CMV-transfected controls. (**C**) Titration of p107-mediated suppression in wild-type versus mutant Gal-Myc constructs. NIH 3T3 cells were transfected as in (B) with increasing ratios of CMV-p107:Gal-Myc plasmids. Values are expressed as in (B). Experiments were done in duplicate and the average value is shown.

tion factor complex TFIID (*25*), p107 may suppress Myc-driven transcription by preventing Myc-TFIID association. The mechanism by which mutations in Myc prevent suppression by p107 also remains to be elucidated.

Taken together, the interaction between Myc and p107 shown here and the ubiquitous expression of both these proteins have implications for the mechanisms regulating cell cycle progression in mammalian cells. When overexpressed, p107 inhibits cell proliferation by blocking the cell cycle before S phase (*11, 12*). Unlike the situation with Rb, however, the p107-mediated growth arrest cannot be rescued by cyclin A, cyclin E, or E2F1 (*12, 26*), suggesting that p107 targets other cell cycle progression factors. The results of this study indicate that Myc may be one of these factors and suggest that the growth-inhibitory activity of p107 may be mediated through suppression of Myc-Max transcriptional complexes. This notion is consistent with the observation that Myc is rapidly synthesized when cells enter G1 (*1*), a stage of the cell cycle when p107 is also present in various transcription complexes (*27*). We have also shown that Rb does not bind Myc; hence our results indicate that the highly related p107 and Rb proteins regulate different targets during the cell cycle.

The observation that tumor-associated mutant forms of Myc escape suppression by p107 provides insight in the mechanisms leading to *myc* oncogene activation in BL. In these tumors, *myc* transcriptional regulation is disrupted by chromosomal translocations that juxtapose the gene to heterologous promoter elements (*23*). We suggest that mutations within the transcriptional activation domain may further deregulate Myc activity at the protein level by enabling it to escape p107-mediated modulation. This may be a common mechanism for Myc deregulation, as mutations analogous to those observed in BL have been detected in tumor types that do not exhibit *myc* translocations (*28*). Overproduction of Myc by gene amplification, a common aberration in various tumor types (*1*), or by p107 loss or inactivation, are other mechanisms by which the Myc could escape regulation by p107 in tumor cells.

REFERENCES AND NOTES

1. B. Luscher and R. N. Eisenman, *Genes Dev.* **4**, 2025 (1990); K. B. Marcu, S. A. Bossone, A. J. Patel, *Annu. Rev. Biochem.* **61**, 809 (1992).
2. E. M. Blackwood and R. N. Eisenman, *Science* **251**, 1211 (1991); E. M. Blackwood, B. Luscher, R. N. Eisenman, *Genes Dev.* **6**, 71 (1992); G. J. Kato, W. M. F. Lee, L. Chen, C. V. Dang, *ibid.*, p. 81.
3. L. Kretzner, E. M. Blackwood, R. N. Eisenman, *Nature* **359**, 426 (1992); B. Amati *et al.*, *ibid.*, p. 423.
4. W. Gu, K. Cechova, V. Tassi, R. Dalla-Favera, *Proc. Natl. Acad. Sci. U.S.A.* **90**, 2935 (1993).
5. D. E. Ayer, L. Kretzer, R. N. Eisenman, *Cell* **72**, 211 (1993); D. E. Ayer and R. N. Eisenman, *Genes Dev.* **7**, 2110 (1993).
6. G. I. Evan *et al.*, *Cell* **69**, 119 (1992); Y. Shi *et al.*, *Science* **257**, 212 (1992).
7. S. Chellappan, S. Hiebert, M. Mudryj, J. Horowitz, J. Nevins, *Cell* **65**, 1053 (1991); S. W. Hiebert, S. P. Chellappan, J. M. Horowitz, J. R. Nevins, *Genes Dev.* **6**, 177 (1992); M. Zamanian and N. B. La Thangue, *EMBO J.* **11**, 2603 (1992); B. M. Herchbach and A. D. Johnson, *Annu. Rev. Cell Biol.* **9**, 479 (1993).
8. A. K. Rustgi, N. Dyson, R. Bernards, *Nature* **352**, 541 (1991); C. Cziepluch, A. Wenzel, J. Schurmann, M. Schwab, *Oncogene* **8**, 2833 (1993).
9. K. Bhatia *et al.*, *Nature Genet.* **56** (1993); T. Yano *et al.*, *Oncogene* **8**, 2741 (1993); J. Murphy and R. Dalla-Favera, unpublished observations.
10. We constructed the FLAG-HMK-Myc plasmid by inserting a 660–base pair (bp) fragment (corresponding to amino acids 1 to 210) of a human *myc* cDNA into the Eco RI cloning site of the FLAG-HMK plasmid vector (*29*). The *myc* fragment was generated by the polymerase chain reaction (PCR) with the following primers: 5′-ATTTGAATTCCCCCTCAACGTTAGCTTCACC-3′ and 5′-ATTTGAATTCTTACGAGGCGCAGGACTTGGGCGAGCT-3′. After subcloning, the *myc* insert and insert-vector junctions were verified by DNA sequence analysis, and the fusion protein was purified and labeled as described (*29*). The Daudi λ-gt11 expression library (Clontech) was derived from polyadenylated RNA from Daudi cells. The phage were plated, filters pretreated with isopropyl β-D-thiogalactopyranoside (IPTG) were placed over the plaques, and the proteins were allowed to transfer overnight at 37°C (*2, 5*). Filters were then blocked with buffer A [5% nonfat dry milk, 20 mM Hepes (pH 7.5), 150 mM KCl, 10 mM $MgCl_2$, 1 mM dithiothreitol (DTT), and 0.1% NP-40] and incubated with ^{32}P-labeled FLAG-HMK-Myc probe (2×10^8 cpm; ~20 nM protein) in buffer B [1% nonfat dry milk, 20 mM Hepes (pH 7.5), 150 mM KCl, 10 mM $MgCl_2$, 10 mM DTT, 0.1% NP-40, and 10% glycerol] for 6 to 8 hours. Filters were then washed in buffer B three times (25 min each). All procedures were done at 4°C. Filters were then subjected to autoradiography.
11. M. E. Ewen *et al.*, *Cell* **58**, 257 (1989); M. E. Ewen, Y. Xing, J. B. Larence, D. M. Livingston, *ibid.* **66**, 1155 (1991).
12. L. Zhu *et al.*, *Genes Dev.* **7**, 1111 (1993); Q. J. Hu, N. Dyson, E. Harlow, *EMBO J.* **9**, 1147 (1990); X. Q. Qin, T. Chittenden, D. Livingston, W. G. Kaelin, *Genes Dev.* **6**, 953 (1992).
13. L. Lombardi, E. W. Newcomb, R. Dalla-Favera, *Cell* **49**, 101 (1987); F. Grignani, L. Lombardi, G. Inghirami, R. Dalla-Favera, *EMBO J.* **9**, 3913 (1990).
14. Cells (3×10^7) were washed twice with cold phosphate-buffered saline (PBS), incubated in lysis buffer [40 mM tris-HCl (pH 8.0), 150 mM NaCl, 10% glycerol, 1 mM vanadate, 1 mM $ZnCl_2$, 10 mM NaF, 0.5% aprotinin, 0.1% leupeptin, 1 mM phenylmethylsulphonyl fluoride (PMSF), and 0.2% NP-40], and subjected to mild sonication. Cell extracts were then centrifuged for 30 min at 12,000*g* at 4°C, and the indicated antibodies were added and incubated for 2 hours at 4°C. The antibodies to Myc and Rb were from UBI; all other antibodies were gifts (*16*). The immune complexes were collected on protein A–Sepharose beads (Pharmacia), washed five times with lysis buffer, solubilized by Laemmli sample buffer, and subjected to electrophoresis through 7.5% SDS-polyacrylamide gels. The separated proteins were transferred to nitrocellulose filters, which were incubated first in blocking buffer [5% nonfat milk in PBS-T (PBS plus 0.05% Tween 20)] for 3 hours at room temperature and then with antibody (diluted 1:1000 with PBS-T) for 6 to 8 hours at 4°C. The filters were washed three times in PBS-T, incubated with horseradish peroxidase–conjugated sheep antibody to rabbit immunoglobulin G (Amersham; diluted 1:2000 with PBS-T) for 1 hour at room temperature, and then washed and developed by an enhanced chemiluminescence reaction kit (ECL, Amersham).
15. The blot shown in Fig. 2A was stripped and reported with an antibody to Rb. Rb-p110 was detectable in immunoprecipitates generated by the antibody to Rb, but not in those generated by other antibodies or control serum (*16*).
16. W. Gu and R. Dalla-Favera, unpublished results.
17. Bjab is derived from a B cell lymphoma and contains normal *myc* alleles; EW-36 is derived from a Burkitt lymphoma and contains a translocated *myc* allele with normal coding sequences (*9*).
18. G. J. Kato, W. M. F. Lee, C. V. Dang, *Mol. Cell. Biol.* **10**, 5914 (1990).
19. We constructed the Gal-Myc expression plasmid by inserting a 660-bp *myc* fragment (corresponding to amino acids 1 to 210) into the Bam HI–Sal I cloning site of the Gal-0 vector (*15*). The *myc* fragment was generated from human *myc* cDNA (*4*) by PCR. The following primers were used to generate terminal Bam HI–Sal I sites: 5′-AAGGGGATCCCCCTCAACGTTAGCTTCACC-3′ and 5′-AAGGGTCGACTTACGAGGCGCAGGACTTGGGCGA-3′. The other Gal-based constructs were described (*15, 17*), as was the CMV-p107 plasmid (*12*). NIH 3T3 cells were transfected in 100-mm plates (5×10^5 cells per plate) by the calcium phosphate procedure (*4, 15*). The total amount of transfected DNA (20 μg) was kept constant in each experiment by the addition of vector plasmids. Plasmid (2 μg) containing the bacterial β-galactosidase gene was also cotransfected in each experiment to serve as an internal control for transfection efficiency. At 48 hours after transfection, cells were harvested and transcriptional activation was assayed as CAT activity.
20. A. Seth, E. Alvarez, S. Gupta, R. J. Davis, *J. Biol. Chem.* **266**, 23521 (1991); A. Seth, S. Gupta, R. Davis, *Mol. Cell. Biol.* **13**, 4125 (1993).
21. The protein p107 was able to suppress the transactivation activity of two Gal-Myc deletion mutants (amino acids 1 to 103 and 41 to 143) that define the minimal Myc region (amino acids 41 to 103) sufficient for transactivation (*16, 18*).
22. The amino acid mutations in Myc from the three BL cell lines were as follows. P3HR1: 39, 57, 98, 129; ST486: 36, 57, 95; and CA46: 54, 57, 60, 85 (*9*). The Gal-Myc constructs containing the three mutated alleles were prepared as described for the wild-type allele (*16*), except that the Myc inserts were generated by PCR from plasmids (pMYC-P3HR1, pMYC-ST486, and pMYC-CA46) containing the appropriate genomic sequences.
23. R. Dalla-Favera, in *Causes and Consequences of Chromosomal Translocations*, I. Kirsch, Ed. (CRC Press, Boca Raton, FL, 1993), pp. 313–321.
24. S. J. Weintraub, C. A. Prater, D. C. Dean, *Nature* **358**, 259 (1992).
25. J. Hateboer *et al.*, *Proc. Natl. Acad. Sci. U.S.A.* **90**, 8489 (1993).
26. M. E. Ewen, B. Faha, E. Harlow, D. M. Livingston, *Science* **255**, 85 (1992); B. Faha, M. E. Ewen, L.-H. Tsai, D. M. Livingston, E. Harlow, *ibid.*, p. 87; L. Cao *et al.*, *Nature* **355**, 176 (1992).
27. J. Schwarz *et al.*, *EMBO J.* **12**, 1013 (1993).
28. K. Bhatia and I. T. Magrath, unpublished results. Point mutations in the second exon of *myc* analogous to those detected in BL have been detected in multiple myeloma and small-cell lung cancer samples.
29. M. A. Blanar and W. J. Rutter, *Science* **256**, 1014 (1992).

30. We thank S. Chellapan for a polyclonal antibody to p107 and helpful discussions; M. Ewen and L. Zhu for wild-type and mutant p107 plasmids; N. Dyson for a monoclonal antibody to p107; R. Eisenman for polyclonal antibodies to Max; and K. P. Leclair for the FLAG-HMK plasmid. Supported by NIH grants CA 37165 (to R.D.-F.) and CA 51497 (to C.V.D.). C.V.D. is a Scholar of the Leukemia Society of America.

28 December 1993; accepted 7 March 1994